

Searches for additional Higgs bosons in multi-top-quarks events at the LHC and the International Linear Collider

Shinya Kanemura,^{1,*} Hiroshi Yokoya,^{1,2,†} and Ya-Juan Zheng^{3,‡}

¹*Department of Physics, University of Toyama, Toyama 930-8555, Japan*

²*Theory Center, KEK, Tsukuba 305-0801, Japan*

³*CTS, CASTS and Department of Physics,
National Taiwan University, Taipei 10617, Taiwan*

(Dated: March 4, 2022)

Abstract

We study direct searches of additional Higgs bosons in multi-top-quarks events at the LHC Run-II, its luminosity upgraded version with 3000 fb^{-1} , and the International Linear Collider (ILC) with the collision energy of 1 TeV. Additional Higgs bosons are predicted in all kinds of extended Higgs sectors, and their detection at collider experiments is a clear signature of the physics beyond the standard model. We consider two Higgs doublet models with the discrete symmetry as benchmark models. If these additional Higgs bosons are heavy enough, the decay modes including top quarks can be dominant, and the searches in multi-top-quarks events become an important probe of the Higgs sector. We evaluate the discovery reach in the parameter space of the model, and find that there are parameter regions where the searches at the LHC with 3000 fb^{-1} cannot survey, but the searches at the ILC 1 TeV run can. The combination of direct searches at the LHC and the ILC is useful to explore extended Higgs sectors.

PACS numbers: 12.60.Fr, 13.66.Hk, 14.80.Ec, 14.80.Fd,

* kanemu@sci.u-toyama.ac.jp

† hyokoya@sci.u-toyama.ac.jp

‡ yjzheng218@gmail.com

I. INTRODUCTION

A Higgs boson (h) was discovered at the LHC Run-I in 2012 [1, 2]. After the discovery, further precision measurements have revealed its properties, which seem to be quite consistent with those of the Higgs boson in the standard model (SM) within current experimental errors [3–6]. By measuring the mass of the Higgs boson very precisely, $m_h = 125.09 \pm 0.24$ GeV at the LHC [7], the parameters in the Higgs potential in the SM have been determined experimentally. However, the whole structure of the Higgs sector is still unclear, since one can consider models with extra scalar fields, like the Higgs sector in the supersymmetric models, satisfying all the available constraints including the properties of the discovered h . Moreover, in fact, numbers of models with extra scalar fields have been proposed to solve the problems which cannot be explained within the SM, such as neutrino masses, dark matter, baryon asymmetry of the universe, cosmic inflation, etc. Determining the structure of the Higgs sector experimentally becomes an important foothold in constructing the new theory above the electroweak scale.

For this purpose, further precision measurements are required to pin down small deviations from the SM in the properties of h [8, 9]. This shall be performed at the LHC Run-II with increased energy and more accumulated luminosity, and also at the future lepton colliders, such as the International Linear Collider (ILC) [10, 11], the Future Circular Collider (FCC) [12], and the Compact Linear Collider (CLIC) [13]. By measuring deviations from the SM in the properties of h , one can probe an extended Higgs sector with rather large masses of additional Higgs bosons so that effects by the extended part in the Higgs sector tend to decouple from the properties of the SM-like h [14, 15].

Another approach to elucidate the whole structure of the Higgs sector is to directly search for additional Higgs bosons, since their existence must be a clear evidence of an extended Higgs sector. Direct searches of additional Higgs bosons have been performed at the LHC Run-I in various decay modes [16], and the limits on the mass of additional Higgs bosons and their coupling strength have been investigated. On the prospect of the direct searches at future colliders, the LHC Run-II has an advantage since it is the energy frontier experiment which is good to produce heavier particles. However, on the other hand, direct searches at the ILC have a different advantage, that is, a parameter regions with relatively small cross section can be probed due to the clean environment of lepton collider experiments, although

the mass reach for additional Higgs bosons is relatively limited. Thus, the searches at the LHC Run-II or its luminosity upgraded version with 3000 fb^{-1} (LHC 3000 fb^{-1}) and the ILC can be complementary to survey the wide parameter regions in extended Higgs sectors [17].

In this paper, we study multi-top-quarks events as distinct signals of production of additional Higgs bosons. As benchmark models of extended Higgs sectors, we consider two Higgs doublet models (2HDMs).¹ In the 2HDM, there are CP -even H , CP -odd A , and a pair of charged H^\pm in addition to the SM-like h . For neutral H and A , the decays into a top-quark pair open if their masses are larger than about 350 GeV. Because of the large mass of the top quark, it is quite possible that this decay mode dominates the branching fraction at least in certain regions in the parameter space. Thus, the multi-top-quarks events can be an attractive signal of the heavy Higgs bosons. Such multi-top-quarks events have been studied at the LHC as a signal of new particle in various models [20–34]. A large production rate of multi-top-quarks events is predicted at the LHC for the models with colored new particles such as gluinos, color-octet scalars, etc., but that for non-colored particles such as heavy additional Higgs bosons is limited. At the ILC, four top-quarks production can be considered as a signal of H and A , through $e^+e^- \rightarrow HA$ and $e^+e^- \rightarrow f\bar{f}H/A$ [17, 35, 36]. To produce a pair of H and A which decay into top-quark pairs, both the masses of H and A are required to be larger than about 350 GeV, and the collision energy should be higher than about 700 GeV. Such an experiment can be realized at the ILC with $\sqrt{s} = 1 \text{ TeV}$. Up to our knowledge, there has been no dedicated study on this process at lepton colliders. Therefore, in this paper, we aim to present a detailed analysis on this process including the hadron-level simulation with jet clustering, flavor tagging, detector acceptance and momentum resolution effects. We find that the four top-quarks events can be detected by simple kinematical cuts, and thus be useful to survey the parameter regions in the 2HDM. We note that the signal of heavy charged Higgs boson can be $H^\pm \rightarrow t\bar{b}(\bar{t}b)$, and its observability has been studied in $gb \rightarrow tH^\pm$ process at hadron colliders [37, 38], and also at lepton colliders in $e^+e^- \rightarrow H^+H^-$ and $e^+e^- \rightarrow H^\pm f\bar{f}'$ [39–41].

The paper is organized as follows. In Sec. II, we briefly introduce the 2HDM with Z_2 symmetry considering the four types of Yukawa interactions. In Sec. III, we present an analysis for the search prospect of additional Higgs bosons in multi-top-quarks events at the LHC. In Sec. IV, we study the four top-quarks events at the ILC by performing the

¹ For the review of the 2HDMs, see, e.g., Refs. [18, 19].

	Φ_1	Φ_2	u_R	d_R	ℓ_R	Q_L	L_L
Type-I	+	-	-	-	-	+	+
Type-II	+	-	-	+	+	+	+
Type-X	+	-	-	-	+	+	+
Type-Y	+	-	-	+	-	+	+

TABLE I. Four possible Z_2 charge assignments to the scalar and fermion fields.

Monte-Carlo simulation for the signal and background processes at the hadron level with detector effects. By using the simulation analysis, we evaluate the discovery potential of the neutral Higgs bosons at the ILC in the four top-quarks events in the parameter space in the 2HDM with four types of Yukawa interactions. The obtained discovery reaches at the LHC and at the ILC are compared. Sec. V is devoted to discussions for further investigation and future prospects. Finally, we draw a conclusion in Sec. VI.

II. TWO HIGGS DOUBLET MODEL

In this section, we briefly introduce the model we consider, namely the 2HDM with the softly-broken Z_2 symmetry. We introduce two isospin doublet scalar fields, Φ_1 and Φ_2 , which transform as $\Phi_1 \rightarrow +\Phi_1$ and $\Phi_2 \rightarrow -\Phi_2$ under the Z_2 transformation. For the SM fermions, there are four kinds of Z_2 parity assignment [42–44], as listed in Table I. We denote the four types of Yukawa interactions as Type-I, Type-II, Type-X and Type-Y [44]. The Yukawa interaction to the SM fermions in each flavor is allowed for only one Higgs field, Φ_1 or Φ_2 , to make each interaction term Z_2 invariant. It forbids the flavor changing neutral currents at the tree-level [45], which are severely constrained by experimental observations.

After solving the condition for the electroweak symmetry breaking and diagonalizing the mass matrices in the Higgs sector assuming CP -invariance, there are five physics scalar states; namely, two CP -even neutral Higgs boson h and H , one CP -odd neutral Higgs boson A , and a pair of charged Higgs bosons H^\pm . The lighter CP -even h can be identified as the SM-like Higgs boson which was observed at the LHC. Yukawa interactions are given

	ξ_h^u	ξ_h^d	ξ_h^ℓ	ξ_H^u	ξ_H^d	ξ_H^ℓ	ξ_A^u	ξ_A^d	ξ_A^ℓ
Type-I	c_α/s_β	c_α/s_β	c_α/s_β	s_α/s_β	s_α/s_β	s_α/s_β	$\cot \beta$	$-\cot \beta$	$-\cot \beta$
Type-II	c_α/s_β	$-s_\alpha/c_\beta$	$-s_\alpha/c_\beta$	s_α/s_β	c_α/c_β	c_α/c_β	$\cot \beta$	$\tan \beta$	$\tan \beta$
Type-X	c_α/s_β	c_α/s_β	$-s_\alpha/c_\beta$	s_α/s_β	s_α/s_β	c_α/c_β	$\cot \beta$	$-\cot \beta$	$\tan \beta$
Type-Y	c_α/s_β	$-s_\alpha/c_\beta$	c_α/s_β	s_α/s_β	c_α/c_β	s_α/s_β	$\cot \beta$	$\tan \beta$	$-\cot \beta$

TABLE II. The scaling factors ξ_ϕ^f for the four types of Yukawa interactions [44]. $c_\theta = \cos \theta$, and $s_\theta = \sin \theta$ for $\theta = \alpha, \beta$.

in terms of these physical scalars as

$$\begin{aligned}
-\mathcal{L}_{\text{Yukawa}} = & \sum_{f=u,d,\ell} \left[\frac{m_f}{v} \xi_h^f \bar{f} f h + \frac{m_f}{v} \xi_H^f \bar{f} f H - i \frac{m_f}{v} \xi_A^f \bar{f} \gamma_5 f A \right] \\
& + \left\{ \frac{\sqrt{2} V_{ud}}{v} \bar{u} [m_u \xi_A^u P_L + m_d \xi_A^d P_R] d H^+ + \frac{\sqrt{2} m_\ell}{v} \xi_A^\ell \bar{\nu}_L \ell_R H^+ + \text{H.c.} \right\}, \quad (1)
\end{aligned}$$

where the scaling factor ξ_ϕ^f with $\phi = h, H, A$ and $f = u, d, \ell$ can be found in Table II. The scaling factor is a function of α and β , the mixing angles in the neutral CP -even component and CP -odd component, respectively. The mixing angle β also satisfies $\tan \beta = v_2/v_1$, where v_1 and v_2 are the vacuum expectation values of the two doublet fields.

The gauge coupling of h is given by $g_{hVV}^{2HDM} = g_{hVV}^{\text{SM}} \sin(\beta - \alpha)$ and that of H is given by $g_{HVV}^{2HDM} = g_{hVV}^{\text{SM}} \cos(\beta - \alpha)$. Theoretically, a deviation of $\sin(\beta - \alpha)$ from unity is constrained by the arguments of perturbative unitarity [46–48] and vacuum stability [49–51]. If a soft-breaking scale of the Z_2 symmetry M is larger than the electroweak scale, $M \gg v$, only small value of $1 - \sin(\beta - \alpha)$ is allowed by these constraints [52]. The limit of $\sin(\beta - \alpha) \rightarrow 1$ is called the SM-like limit, where h has the same coupling constants to the gauge bosons and also to the SM fermions as the SM Higgs boson. On the other hand, Yukawa interactions of H, A and H^\pm to the SM fermions do not vanish in this limit, and the coupling strength for each vertex depends on the type of Yukawa interactions and $\tan \beta$. Thus, the variety of the type of Yukawa interactions with different $\tan \beta$ dependences leads to rich phenomenology for the additional Higgs bosons.

We focus on the interactions of additional Higgs bosons to top quarks. For any type of Yukawa interactions, the Yukawa coupling constants to top quarks are enhanced by $\cot \beta$ for small $\tan \beta$ regions. Therefore, for larger masses of additional Higgs bosons where the decay

modes into top quarks are open, the branching ratio to top quarks becomes dominant for small $\tan\beta$ regions. The figures for the branching ratio of additional Higgs bosons can be found, e.g., in Refs. [14, 17]. For larger $\tan\beta$, the dominant branching ratio is replaced by the other fermionic mode, $b\bar{b}$ for Type-II and Type-Y, $\tau^+\tau^-$ for Type-X Yukawa interactions. For Type-I, since the $\tan\beta$ dependence is common for all fermions, the dominance of $t\bar{t}$ decay mode is true for any value of $\tan\beta$.

III. MULTI-TOP-QUARKS PRODUCTION AT THE LHC

In this section, we study the four top-quarks production through the production of additional Higgs boson(s) at the LHC. The largest contribution comes from the top-quark pair associated production process,

$$pp \rightarrow t\bar{t}H(t\bar{t}A) \rightarrow t\bar{t}t\bar{t}, \quad (2)$$

since it emerges via the strong interaction. At the tree level, there are two subprocesses in this process. One is $gg \rightarrow t\bar{t}H(t\bar{t}A)$ and the other is $q\bar{q} \rightarrow t\bar{t}H(t\bar{t}A)$. Because $H(A)$ is radiated off from the top quarks, the cross section is proportional to the square of y_t^H (y_t^A) which is proportional to $\cot\beta$ in the SM-like limit. Therefore, the cross section is large for smaller $\tan\beta$.

The four top-quarks production through the pair production of H and A ,

$$pp \rightarrow HA \rightarrow t\bar{t}t\bar{t}, \quad (3)$$

is described by the quark anti-quark annihilation process, $q\bar{q} \rightarrow Z^* \rightarrow HA$ at the tree level. Since the HA production cross section does not depend on $\tan\beta$, the cross section of the final four top-quarks production depends on $\tan\beta$ through the branching ratios of H and A into the top-quark pair, $\mathcal{B}^{H/A}(t\bar{t})$.

There are also three top-quarks production processes via the associated production of H^\pm and $H(A)$, which subsequently decay into $t\bar{b}(\bar{t}b)$ and $t\bar{t}$, respectively,

$$pp \rightarrow H^\pm H(H^\pm A) \rightarrow t\bar{b}\bar{t}/\bar{t}b t\bar{t}. \quad (4)$$

At the tree level, this production process is described by the W boson mediated diagram [53, 54],

$$q\bar{q}' \rightarrow W^* \rightarrow H^\pm H(H^\pm A). \quad (5)$$

We estimate the cross sections for these processes at the LHC at the tree level. As an example, we take the 2HDM with Type-II Yukawa interactions. For simplicity, we take a common mass for all the additional Higgs bosons. Our calculation is performed with the use of analytic equations in Ref. [55] and the numerical codes generated by `MadGraph5` [56]. To calculate the branching fractions of $H \rightarrow t\bar{t}$ and $A \rightarrow t\bar{t}$, the off-shell effect of top quarks is included. To estimate the hadronic cross section, the `CTEQ6L` parton distribution functions (PDFs) [57] are used with setting the scale of PDFs to $\mu_F = m_{\Phi_1} + m_{\Phi_2}$ for HA and $H^\pm H + H^\pm A$ production processes, and to $\mu_F = m_t + m_\Phi/2$ for the $t\bar{t}H(A)$ production process [55]. In Fig. 1, the results are plotted as a function of the mass for the LHC 8 TeV (left) and the LHC 14 TeV (right). The cross sections for $t\bar{t}H + t\bar{t}A$, HA and $H^\pm H + H^\pm A$ productions are plotted in blue, black and red dotted lines, respectively. For the $t\bar{t}H + t\bar{t}A$ production process, the results for $\tan\beta = 1$ and 3 are plotted. In addition, the resulting cross sections for the multi-top-quark production processes are plotted in solid (dashed) lines with the same color, assuming that $\tan\beta = 1$ and 3. The cross sections at 13 TeV collision energy are about 70-80% of those at 14 TeV.

For each process, the largest cross section is realized for the mass of additional Higgs bosons at around 350 GeV. Below this value, the branching ratio into $t\bar{t}$ is suppressed because one of the top quarks is forced to be off-shell, while above that value the production cross sections of additional Higgs bosons get decreased. For $\tan\beta = 1$, the cross section of the four top-quarks production can be at most 6 fb (50 fb) for the LHC 8 TeV (14 TeV). We note that there has been already an experimental upper limit for the cross section of four top-quarks production at the LHC 8 TeV [58, 59]. The CMS Collaboration has set the limit to $\sigma_{4t} \leq 32$ fb at the 95% CL (confidence level) [59], by observing the lepton plus multi-jets events. However, the limit is not tight enough to constrain the parameter regions in the 2HDM. We also note that the SM prediction to the four top-quarks production at the LHC 8 TeV is about 1 fb [24]. For the three top-quarks production, since the expected cross section is smaller than that of four top-quarks production while the signatures mix up with that of four top-quarks production, the detection may be more challenging.

We now study the prospect of measuring four top-quarks production as a signal of the production of additional Higgs bosons at the future LHC run. For the four top-quarks production within the SM contribution, the total cross section and its uncertainty are estimated to be $\sigma_{\text{SM}} = 15$ fb and $\delta\sigma_{\text{SM}} = 4$ fb, respectively [60]. To deal with the background

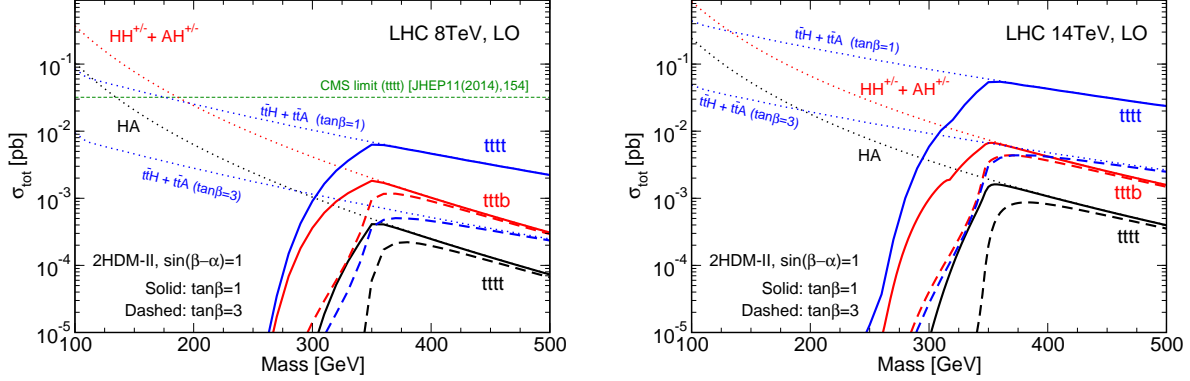


FIG. 1. Cross sections for multi-top-quarks production at the LHC 8 TeV (left) and 14 TeV (right) for the Type-II 2HDM. four top-quarks production from $t\bar{t}H + t\bar{t}A$ production, HA production and three top-quarks production from $HH^\pm + AH^\pm$ production are shown with $\tan\beta = 1$ (solid lines) and 3 (dashed lines).

processes, we follow the analysis in Ref. [22] where the selection cuts to extract the four top-quarks events out of the background events are demonstrated by simulation analysis. In their analysis, the background rate of $B = 7.2$ fb after selection cuts is obtained with the signal efficiency of $\epsilon = 0.03$. By taking into account the statistical and systematical uncertainties for the signal, SM and background processes, the accuracy of measuring the signal cross section σ_S can be estimated as

$$\frac{\delta\sigma_S}{\sigma_S} = \sqrt{\frac{(\sigma_S + \sigma_{SM})\epsilon + B}{\sigma_S^2\epsilon^2\mathcal{L}} + \frac{\delta\sigma_{SM}^2\epsilon^2 + (\delta B)^2}{\sigma_S^2\epsilon^2}}, \quad (6)$$

where δB denotes the systematic uncertainty of the background rate. We take $\delta B = 0.05B$, which may be achieved at the later stage of the LHC experiment. By solving Eq. (6), we obtain that σ_S has to be larger than 25 fb (63 fb) to achieve $\delta\sigma_S/\sigma_S < 0.5$ (0.2) with the integrated luminosity of $\mathcal{L} = 300$ fb $^{-1}$. In our setup, the total uncertainty is dominated by the systematic uncertainty from the background. To reduce the statistical uncertainty smaller than the systematical one, one needs only more than 10 fb $^{-1}$ of the data. Thus, the accuracy will not be improved by accumulating the integrated luminosity up to 3000 fb $^{-1}$, but is limited by the systematical errors. Increased integrated luminosity is, on the other hand, useful to reduce the systematical uncertainty in the backgrounds. If we change our input by $B = 7.2$ fb \rightarrow 3.6 fb or $\epsilon = 0.03 \rightarrow 0.06$, the resulting values are modified to 14 fb (36 fb) for $\delta\sigma_S/\sigma_S < 0.5$ (0.2), respectively. In the ideal case of $\delta B = 0$, the parameter

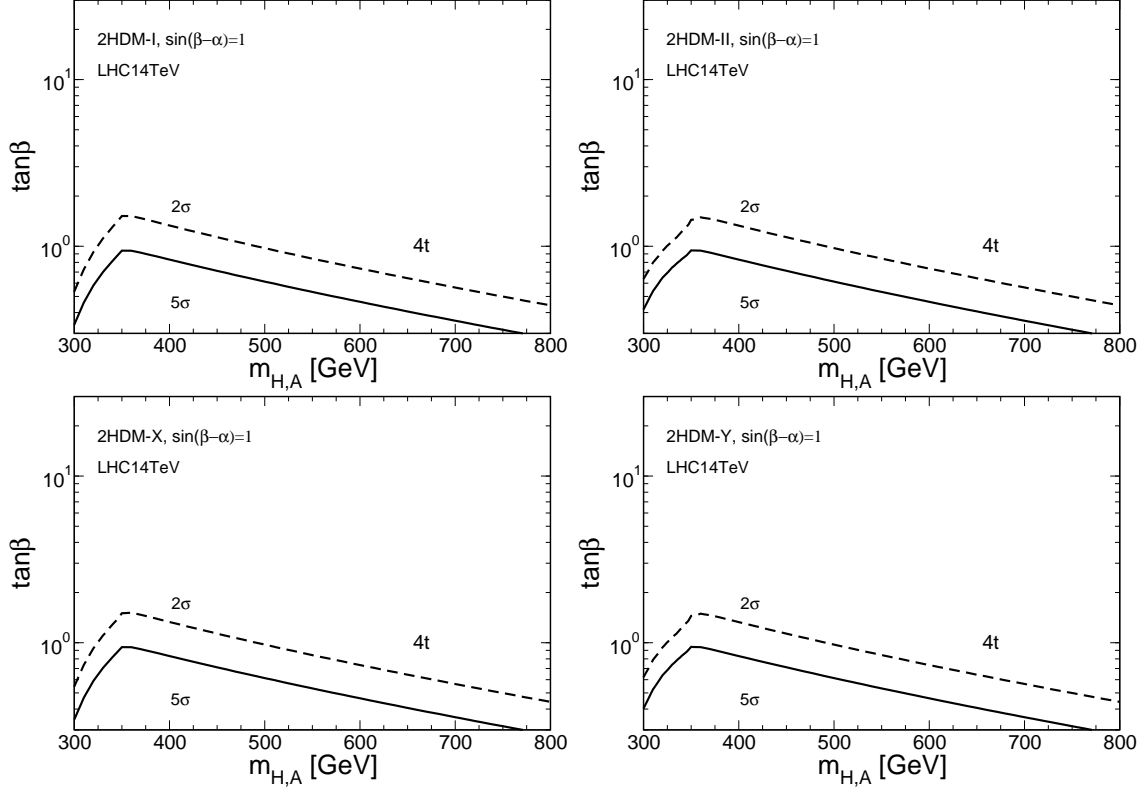


FIG. 2. Contour plot for the discovery reach of four top-quarks events at the LHC Run-II in the 2HDM. Upper limits on $\tan\beta$ for the discovery regions at the 2σ [5σ] CL are shown in dashed [solid] lines.

regions with $\sigma_S \geq 8$ fb (20 fb) can be observed at the 2σ (5σ) CL. To obtain better sensitivity, a considerable amount of efforts to reduce the systematical uncertainties is required.

In Fig. 2, we show the parameter regions in the 2HDM with four types of Yukawa interactions where the additional Higgs bosons contribution can be detected at the LHC in the four top-quarks events at the 2σ and 5σ CL for the above setup. It turned out that the dependence on the type of Yukawa interactions is small, and only $\tan\beta \lesssim 1.5$ can be probed at the 2σ CL at most. Since these regions are constrained by flavor experiments [61, 62], the LHC searches in 4 top-quarks events may not have significant impact on exploring the parameter regions in the 2HDMs.

IV. MULTI-TOP-QUARKS PRODUCTION AT THE ILC

In this section, we consider the four top-quarks production at the ILC. In the 2HDM, the four top-quarks final state is generated via the pair and single production of H and/or A . For $\sqrt{s} > m_H + m_A$, pair production of H and A ,

$$e^+e^- \rightarrow HA, \quad (7)$$

is kinematically possible and its cross section can be sizable. The HA pair production cross section does not depend on $\tan\beta$ at the tree level. Thus, the four top-quarks production rate depends on $\tan\beta$ only through the decay branching ratio of H and A .

On the other hand, for $\sqrt{s} < m_H + m_A$, the pair production is kinematically forbidden, but the single production process

$$e^+e^- \rightarrow t\bar{t}H(t\bar{t}A), \quad (8)$$

can still open as long as $\sqrt{s} > 2m_t + m_{H(A)}$. The cross section of this process can be increased by the enhanced Yukawa coupling of H and A to the top quarks. Followed by the decays of H and A into $t\bar{t}$, four top-quarks events occur from these processes.

Through the decay of top quarks, the signature of four top-quarks production can be observed as all-hadronic, single lepton plus jets plus missing momentum, dilepton plus jets plus missing, trilepton plus jets plus missing, tetralepton plus jets plus missing channels. Among dilepton plus jets plus missing channels, there are same-sign and opposite-sign dilepton final states, where the former is expected to have small backgrounds. The branching fractions for these channels are listed in Table III. In the SM, the leading production mechanism of four top-quarks events is $e^+e^- \rightarrow t\bar{t}g^* \rightarrow t\bar{t}t\bar{t}$ via QCD interactions, thus the cross section is $\mathcal{O}(\alpha^2\alpha_s^2)$. The next-to-leading production mechanism is full electroweak process, $\mathcal{O}(\alpha^4)$. When we consider the final states including the decay of top quarks and their detection at real experiments, there enter reducible backgrounds via $e^+e^- \rightarrow t\bar{t}, t\bar{t}b\bar{b}, t\bar{t}\ell^+\ell^-$, etc. We estimate the contributions from these processes in the following simulation analysis.

First, we describe our simulation analysis for the detection of the 4 top-quarks events at the ILC with $\sqrt{s} = 1$ TeV. We use `MadGraph5` [56] and `Pythia6` [63] for generation of signal and background events, with `Tauola` [64] for tau lepton decays. We evaluate the signal process by including both the single and pair production amplitudes coherently.

Decay modes	Final states	\mathcal{R} (with τ 's)	\mathcal{R} (without τ 's)
all-hadron	$4j_b + 8j$	$(\frac{2}{3})^4 \simeq 0.2$	$(\frac{2}{3})^4 \simeq 0.2$
single lepton + jets	$\ell^\pm + 4j_b + 6j + \nu$	$(\frac{2}{3})^3 \cdot \frac{1}{3} \cdot 4 \simeq 0.4$	$(\frac{2}{3})^3 \cdot \frac{2}{9} \cdot 4 \simeq 0.26$
S.S. dilepton + jets	$\ell^\pm \ell^\pm + 4j_b + 4j + \nu\nu$	$(\frac{2}{3})^2 \cdot (\frac{1}{3})^2 \cdot 2 \simeq 0.1$	$(\frac{2}{3})^2 \cdot (\frac{2}{9})^2 \cdot 2 \simeq 0.04$
O.S. dilepton + jets	$\ell^\pm \ell^\mp + 4j_b + 4j + \nu\nu$	$(\frac{2}{3})^2 \cdot (\frac{1}{3})^2 \cdot 4 \simeq 0.2$	$(\frac{2}{3})^2 \cdot (\frac{2}{9})^2 \cdot 4 \simeq 0.09$
trilepton + jets	$\ell^\pm \ell^\pm \ell^\mp + 4j_b + 2j + \nu\nu\nu$	$\frac{2}{3} \cdot (\frac{1}{3})^3 \cdot 4 \simeq 0.1$	$\frac{2}{3} \cdot (\frac{2}{9})^3 \cdot 4 \simeq 0.03$
tetralepton + jets	$\ell^+ \ell^+ \ell^- \ell^- + 4j_b + \nu\nu\nu\nu$	$(\frac{1}{3})^4 \simeq 0.01$	$(\frac{2}{9})^4 \simeq 2.4 \times 10^{-3}$

TABLE III. Branching fractions of the four top-quarks signature in the decays of top quarks. Branching fractions where ℓ^\pm includes τ^\pm or not are listed.

The SM contribution to the $e^+e^- \rightarrow t\bar{t}\bar{t}\bar{t}$ process is estimated to be very small, giving $\sigma_{\text{tot}} = 3.8 \times 10^{-3}$ fb at $\sqrt{s} = 1$ TeV. Thus, for the integrated luminosity of $\mathcal{L} = 1$ ab $^{-1}$, only a few events are expected to be produced in the SM. The background processes considered in our analysis are

$$e^+e^- \rightarrow t\bar{t}, \quad (9)$$

$$e^+e^- \rightarrow t\bar{t}b\bar{b}, \quad (10)$$

$$e^+e^- \rightarrow t\bar{t}\ell^+\ell^-. \quad (11)$$

$$e^+e^- \rightarrow t\bar{t}W^+W^-. \quad (12)$$

The second process includes $e^+e^- \rightarrow t\bar{t}g^*(\rightarrow b\bar{b})$, $e^+e^- \rightarrow t\bar{t}h(\rightarrow b\bar{b})$, $e^+e^- \rightarrow t\bar{t}Z/\gamma^*(\rightarrow b\bar{b})$, $e^+e^- \rightarrow tbW^*(\rightarrow tb)$, and $e^+e^- \rightarrow W^{*+}W^{*-} \rightarrow t\bar{t}b\bar{b}$. ℓ^\pm in the third process mean the sum of e^\pm , μ^\pm and τ^\pm . The other background processes are negligible.

To analyze the generated events, we follow the designed performance of the ILC detectors [11]. We take all detectable particles whose pseudo rapidity satisfies $|\eta| < 1.5$. For charged particles, we further require their transverse momentum satisfies $p_T > 0.3$ GeV. Four momenta of those particles are smeared by using the Gaussian distribution with $\sigma_{p_T}/p_T = 10^{-4}p_T + 10^{-3}$ for charged particles, $\sigma_E/E = 0.4/\sqrt{E} + 0.02$ for neutral hadrons, and $\sigma_E/E = 0.15/\sqrt{E} + 0.01$ for photons, where p_T and E are given in an unit of GeV.

Among those particles, we select isolated leptons, e and μ , whose energy satisfies $E_{\text{cone}} \leq \sqrt{6(E_\ell - 15)}$ where E_{cone} and E_ℓ are given in an unit of GeV. E_{cone} is the summation of energies of particles inside the cone around the lepton defined as $\cos\theta_{\text{cone}} \geq 0.98$ except the

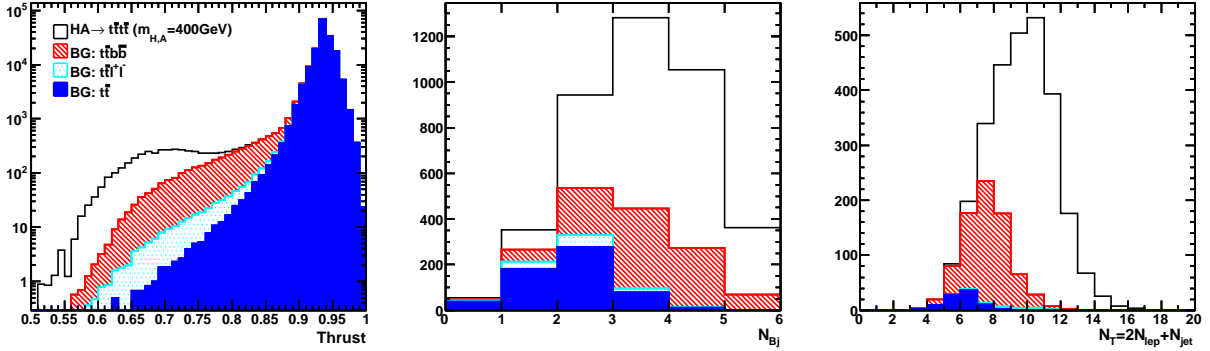


FIG. 3. Kinematical distributions of signal and background events in Thrust (left), N_{bj} (middle), and $N_T = 2N_{lep} + N_{jet}$ (right) variables with loose b -tagging criteria. Signal events are displayed for $m_{H,A} = 400$ GeV with a normalization of $\sigma_{tot} = 2.7$ fb which corresponds to $\tan\beta = 1$ in Type-II 2HDM.

lepton itself [65].

After removing the isolated leptons from the list of particles, we perform a jet clustering by using the Durham algorithm [66] with fixed $Y_{cut} = 5 \times 10^{-4}$ with the help of `Fastjet` [67]. Thus, the number of jets in an event is flexible according to the event structure. For each clustered jet, we perform a flavour tagging. If a jet contains only photons, it is tagged as a *photon-jet*. B -tagging is performed stochastically by using the decay history of particles which is available in the Monte-Carlo simulation. If a jet contains B -hadrons (D -hadrons) in the decay history of constituent particles, we tag it as a *b-jet* randomly with a probability of 80% (10%). A probability of mis-tagging a jet which does not contain B or D -hadrons as a b -jet is set to be 3%. These probabilities correspond to *loose tagging* criteria given in Ref. [11]. We found that this loose criteria works better than rather tight criteria to collect more signal events in the circumstances of small backgrounds. In addition, a jet is tagged as a *tau-jet*, if it contains 1 or 3 charged tracks and satisfies $E_{cone}/E_{jet} > 0.95$ where E_{cone} is the summation of energies inside the small cone around a direction of jet three momenta with $R = 0.15$. The other jets are assumed to be *light-jets*. The number of leptons in an event is counted as $N_{lep} = N_e^{iso} + N_\mu^{iso} + N_{\tau_j}$, where $N_{e(\mu)}^{iso}$ is the number of isolated e (μ) and N_{τ_j} is the number of tau-jets. The number of jets in an event is counted as $N_{jet} = N_{lj} + N_{bj}$, where $N_{lj(bj)}$ is the number of light-jets (b -jets).

Processes	Cross sections	Accumulated efficiencies		
		σ_{tot} [fb]	$T \leq 0.77$	$N_{bj} \geq 3$
$e^+e^- (\rightarrow HA) \rightarrow t\bar{t}\bar{t}$ [Type-II, $\sin(\beta - \alpha) = 1$, $\tan \beta = 1$]				
$m_{H,A} = 360$ GeV	4.3	71%	58%	34%
400 GeV	2.7	92%	74%	43%
440 GeV	1.3	96%	79%	47%
480 GeV	0.30	96%	77%	46%
500 GeV	7.5×10^{-2}	95%	77%	45%
520 GeV	3.2×10^{-2}	95%	77%	45%
560 GeV	1.0×10^{-2}	93%	76%	44%
$e^+e^- \rightarrow t\bar{t}$	166.	3.6×10^{-3}	5.6×10^{-4}	2.0×10^{-6}
$e^+e^- \rightarrow t\bar{t}b\bar{b}$	5.0	19%	14%	0.66%
$e^+e^- \rightarrow t\bar{t}\ell^+\ell^-$	0.76	23%	3.8%	1.4%
$e^+e^- \rightarrow t\bar{t}W^+W^-$	0.14	55%	15%	3.0%
$e^+e^- \rightarrow t\bar{t}\bar{t}$ (SM)	3.8×10^{-3}	93%	74%	41%

TABLE IV. The total cross section and the accumulated efficiencies by kinematical cuts for the signal and background processes at the ILC with $\sqrt{s} = 1$ TeV. Signal cross sections and efficiencies are calculated for $m_{H,A} = 360$ GeV to 560 GeV with $\tan \beta = 1$ for Type-II as a reference.

To extract the signal events out of the SM background, we impose following selection cuts; (1) small thrust, $T < 0.77$, (2) $N_{bj} \geq 3$, and (3) large “*hard multiplicity*”, $N_T \equiv 2N_{\text{lep}} + N_{\text{jet}} \geq 10$. In Fig. 3, we show distributions of signal and background events in thrust, N_{bj} and N_T in the left, middle and right panels, respectively. Backgrounds from $t\bar{t}$, $t\bar{t}\ell^+\ell^-$, and $t\bar{t}b\bar{b}$ productions are shown in blue, cyan, and red histograms, respectively. Contributions from the $t\bar{t}W^+W^-$ process and the SM four top-quarks production are omitted since these are small enough. For the reference, signal events with $m_{H,A} = 400$ GeV are shown on top of them where the normalization is adjusted to the case of $\tan \beta = 1$ in the Type-II 2HDM. We find that large $t\bar{t}$ backgrounds are excluded by the thrust cut, and a large amount of $t\bar{t}$, $t\bar{t}\ell^+\ell^-$ contributions is excluded by the N_{bj} cut. Furthermore, all the backgrounds are suppressed by applying the cut on N_T .

The background reduction and signal detection efficiencies are summarized in Table IV

where the background process Eq. (12) and the SM four top-quarks production processes are also included for the reference. In our simulation, the background reduction rates by the above three cuts are $\mathcal{O}(10^{-6})$ for $t\bar{t}$, 0.66% for $t\bar{t}b\bar{b}$, 1.4% for $t\bar{t}\ell^+\ell^-$, and 3% for $t\bar{t}W^+W^-$. With the integrated luminosity of $\mathcal{L} = 1 \text{ ab}^{-1}$, only around 47.8 events are expected to be observed. From the SM four top-quarks production, we expect 1.6 events. On the other hand, for the signal process of additional Higgs bosons, around 34% to 47% of events are remained after these cuts, depending on the mass.

By using the signal detection efficiency ϵ_S with the expected number of background rate $B = 49.4 \text{ ab}$ at $\mathcal{L} = 1 \text{ ab}^{-1}$, we can estimate the minimum value of the total cross section for the signal process to be identified in a certain accuracy. We take into account only the statistical uncertainties due to the presence of backgrounds, since at lepton colliders systematical uncertainties can be expected to be well under control. Thus, the uncertainty of observing the total cross section of signal events is estimated as

$$\frac{\delta\sigma_S}{\sigma_S} = \sqrt{\frac{\sigma_S\epsilon_S + B}{\sigma_S^2\epsilon_S^2\mathcal{L}}}. \quad (13)$$

We find that the signal process can be detected at the 2σ (5σ) CL if the total cross section is above 0.034-0.048 fb (0.11-0.15 fb), depending on the mass of additional Higgs bosons through the signal detection efficiency.

In Fig. 4, we evaluate the parameter regions in the $(m_{H,A}, \tan\beta)$ plane in the 2HDMs where the four top-quarks events can be detected at the ILC. Solid (dashed) contours show the regions where the signal can be detected at the 2σ (5σ) CL. For Type-II and Type-Y 2HDM, $\tan\beta$ up to around 7 (6) can be probed for the mass of additional Higgs bosons up to $m_{H,A} \lesssim 500 \text{ GeV}$. Above $m_{H,A} \simeq 500 \text{ GeV}$, the signal can be produced by using the single Higgs production processes, Eq. (8), but only visible for small $\tan\beta$ below unity. For Type-X 2HDM, $\tan\beta$ up to around 15 (12) can be probed for $m_{H,A} \lesssim 500 \text{ GeV}$, because of the fact that the $H/A \rightarrow t\bar{t}$ decay branching rate remains to be dominant up to larger $\tan\beta$ than that in Type-II and Y. For Type-I 2HDM, since the $H/A \rightarrow t\bar{t}$ decay mode dominates for any value of $\tan\beta$, the four top-quarks events can be observed for any value of $\tan\beta$, as long as $m_{H,A} \lesssim 500 \text{ GeV}$.

We note that, however, the result for Type-I is due to the fact that we take the SM-like limit, $\sin(\beta - \alpha) = 1$, where no $H \rightarrow WW, ZZ, hh$ or $A \rightarrow Zh$ decay is induced. For example, if we take $\sin(\beta - \alpha) = 0.99$, these decay modes become non-zero, and even

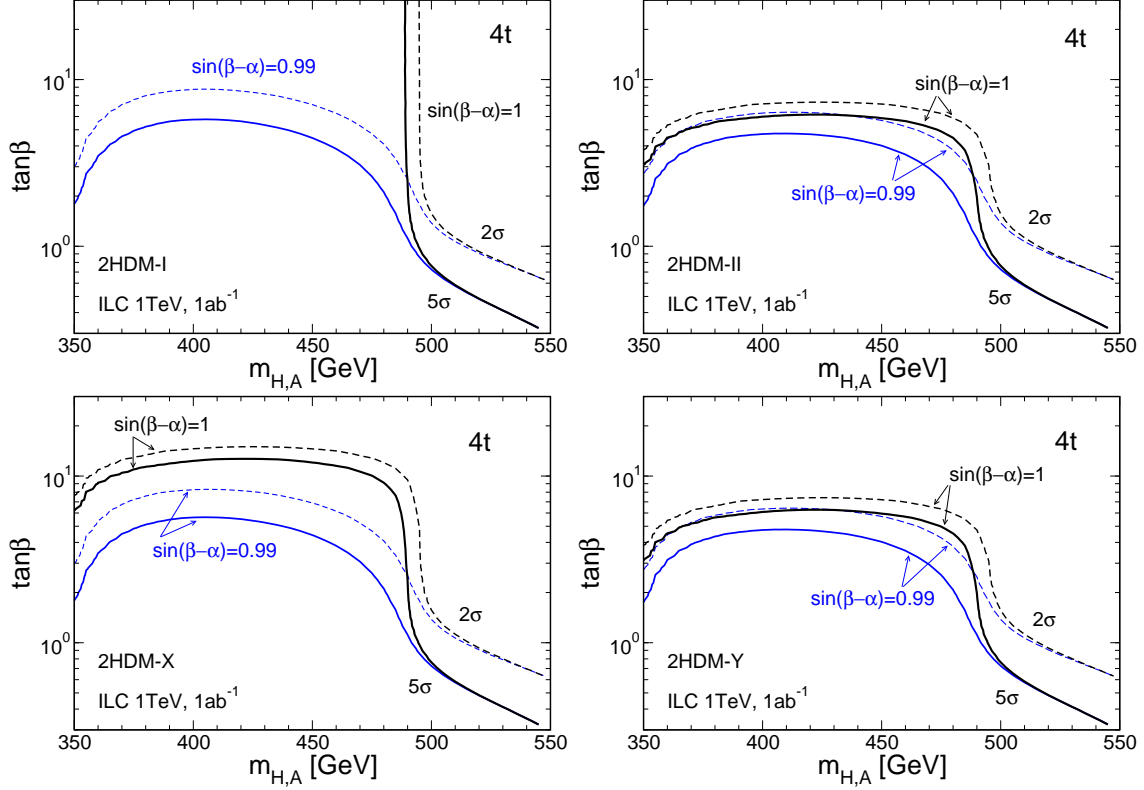


FIG. 4. Contour plot of the discovery reach of the four top-quarks production in the 2HDMs at the ILC $\sqrt{s} = 1$ TeV with $\mathcal{L} = 1 \text{ ab}^{-1}$ data. Upper limits on $\tan \beta$ for the discovery regions at the 2σ [5σ] CL are shown in solid [dashed] lines. The similar results but for $\sin(\beta - \alpha) = 0.99$ are also shown in blue lines.

dominant for larger $\tan \beta$ [14]. The value of $\sin(\beta - \alpha) = 0.99$ can be detected by the precision measurement of hVV coupling constants at the ILC with $\sqrt{s} = 500$ GeV and $\mathcal{L} = 1.6 \text{ ab}^{-1}$ at the 5σ CL [8]. In this case, the four top-quarks events can be observed up to about $\tan \beta \simeq 8$ (5) at the 2σ (5σ) CL for the four types of Yukawa models. The discovery reaches for $\sin(\beta - \alpha) = 0.99$ are also shown in each figure in Fig. 4 in blue lines.

We now compare the impact of the searches for multi-top-quarks events at the LHC and the ILC on exploring the parameter regions in the 2HDM. At the LHC Run-II, by the searches for four top-quarks events, the parameter regions with $\tan \beta \lesssim 1.5$ can be surveyed in all types of Yukawa interactions. Because the experimental uncertainties are dominated by the systematical ones, the results will not be improved at the LHC 3000 fb^{-1} . On the other hand, at the ILC 1 TeV, we find that the parameter regions with larger $\tan \beta$ can be

surveyed as long as $m_{H,A} \lesssim 500$ GeV. For Type-II and Type-Y (Type-X), the parameter regions with $\tan\beta \simeq 7$ (15) can be explored. For Type-I, because the decay mode into a top-quark pair is dominant for any value of $\tan\beta$, detection of four top-quarks events is anticipated in any value of $\tan\beta$. This result is modified to $\tan\beta \lesssim 9$ in the case of $\sin(\beta - \alpha) = 0.99$. Therefore, the searches for four top-quarks events can explore wider parameter regions at the ILC 1 TeV than at the LHC 3000 fb^{-1} .

V. DISCUSSIONS

In this section, we discuss further investigation on the multi-top-quarks events at the LHC and the ILC, regarding the mass determination of the additional Higgs bosons and the discrimination of the type of Yukawa interactions. In addition, we give some comments on the searches for multi-top-quarks events at future multi-TeV lepton collider, CLIC.

First, we discuss the mass reconstruction of additional Higgs bosons in the decay mode into a top-quark pair. At the LHC, even if some excess in the events for the lepton plus multi-jets channel is observed, the mass reconstruction of additional Higgs boson is difficult, since one has to form an invariant mass of six jets in the pretense of more jets which come from the top quarks and the ISR/FSR jets. The combinatorial uncertainty and the jet energy resolution prevent us from constructing a clear peak in the invariant mass distribution. At the ILC, the mass reconstruction by kinematical methods is still difficult, because of the combinatorial uncertainty and the fact that the top quarks from the decay of additional Higgs bosons with the mass of 350-500 GeV have relatively low velocity. Thus, for the mass determination, we may rely on the other decay modes, accompanied to the $t\bar{t}$ mode, such as $b\bar{b}$ and $\tau^+\tau^-$ [68].

Since the enhancement of the couplings of H and A to top quarks is true for the all four types of Yukawa interactions, the discrimination of the type of Yukawa interactions needs to see the other decay modes, such as $b\bar{b}$ for Type-II and Type-Y and $\tau^+\tau^-$ for Type-II and Type-X. For Type-I, the other decay modes are all suppressed. Therefore, non-observation of the other fermionic channel may be the signature of Type-I.

For the above two reasons, combinations of the searches of additional Higgs bosons in different decay modes are important. Depending on the type of Yukawa interactions and the value of $\tan\beta$, the decay modes into $b\bar{b}$ and $\tau^+\tau^-$ can be explored at the LHC and/or the

ILC [17]. By observing several decay modes and their event rates, $\tan\beta$ can be determined experimentally [69]. In the case of $\sin(\beta - \alpha) < 1$, the decay modes of $H \rightarrow hh, WW, ZZ$, and $A \rightarrow Zh$ can be sizable, especially for Type-I. By the combinations of the measurements of these modes, experimental determination of $\sin(\beta - \alpha)$ may be performed.

Finally, we give some comments on the searches at the CLIC [13]. At the CLIC, the collision energy of multi-TeV, such as 3 TeV, is proposed. With $\sqrt{s} = 3$ TeV, the mass reach would be extended up to about 1.5 TeV. This is totally above the scope at the LHC. Thus, the direct searches at the CLIC would have a great impact in any decay mode of additional Higgs bosons. The top quarks from the decay of such heavier Higgs bosons are more energetic so that the mass reconstruction by using boosted top-jet measurement can be realistic. In the case that H and A are produced with large velocity, the decay products of each Higgs boson are well separated into different hemispheres. Therefore, the mass of additional Higgs boson can be reconstructed by using the invariant mass of all decay products in one hemisphere [70].

VI. CONCLUSIONS

We have studied the direct searches of the additional Higgs bosons in multi-top-quarks events at the future LHC and the ILC experiments. Additional Higgs bosons are predicted in any kind of models with extended Higgs sectors, and the detection of them at colliders is a clear signature of the physics beyond the standard model. As a benchmark model of the extended Higgs sector, we have considered the two Higgs doublet models with discrete symmetry with four types of Yukawa interactions.

At the LHC, the signals of four top-quarks events suffer from systematical uncertainties of estimating the SM backgrounds. Therefore, the searches can only survey the parameter regions with $\tan\beta \lesssim 1.5$ which is disfavored by experimental constraints from flavor physics without adding new particle contents to the model. At the ILC, although the mass reach is almost limited by its beam energy, we have shown that the parameter regions with $\tan\beta \lesssim 8-15$ can be surveyed depending on the type of Yukawa interactions. We have also discussed that further investigation may be performed at the ILC, such as discrimination of the type of Yukawa interactions and determination of the mass of additional Higgs bosons by combining the observations of the other decay modes of H and A in addition to the $t\bar{t}$ mode.

ACKNOWLEDGMENTS

H.Y. thanks Quantum Universe Center at KIAS for the warm hospitality. This work was supported, in part, by Grant-in-Aid for Scientific research from the Ministry of Education, Science, Sports, and Culture (MEXT), Japan, Nos. 22244031, 23104006 and 24340046, and NSC of ROC.

-
- [1] G. Aad *et al.* [ATLAS Collaboration], Phys. Lett. B **716** (2012) 1.
 - [2] S. Chatrchyan *et al.* [CMS Collaboration], Phys. Lett. B **716** (2012) 30.
 - [3] G. Aad *et al.* [ATLAS Collaboration], Phys. Lett. B **726** (2013) 88.
 - [4] G. Aad *et al.* [ATLAS Collaboration], Phys. Lett. B **726** (2013) 120.
 - [5] S. Chatrchyan *et al.* [CMS Collaboration], JHEP **1401** (2014) 096.
 - [6] S. Chatrchyan *et al.* [CMS Collaboration], Phys. Rev. D **89** (2014) 9, 092007.
 - [7] G. Aad *et al.* [ATLAS and CMS Collaborations], arXiv:1503.07589 [hep-ex].
 - [8] D. M. Asner, T. Barklow, C. Calancha, K. Fujii, N. Graf, H. E. Haber, A. Ishikawa and S. Kanemura *et al.*, arXiv:1310.0763 [hep-ph].
 - [9] S. Dawson, A. Gribsan, H. Logan, J. Qian, C. Tully, R. Van Kooten, A. Ajaib and A. Anastassov *et al.*, arXiv:1310.8361 [hep-ex].
 - [10] G. Aarons *et al.* [ILC Collaboration], arXiv:0709.1893 [hep-ph].
 - [11] T. Behnke *et al.*, arXiv:1306.6329 [physics.ins-det].
 - [12] M. Bicer *et al.* [TLEP Design Study Working Group Collaboration], JHEP **1401** (2014) 164.
 - [13] L. Linssen, A. Miyamoto, M. Stanitzki and H. Weerts, arXiv:1202.5940 [physics.ins-det].
 - [14] S. Kanemura, K. Tsumura, K. Yagyu and H. Yokoya, Phys. Rev. D **90** (2014) 075001.
 - [15] S. Kanemura, M. Kikuchi and K. Yagyu, Nucl. Phys. B **896** (2015) 80.
 - [16] K. A. Olive *et al.* [Particle Data Group Collaboration], Chin. Phys. C **38** (2014) 090001.
 - [17] S. Kanemura, H. Yokoya and Y. J. Zheng, Nucl. Phys. B **886** (2014) 524.
 - [18] J. F. Gunion, H. E. Haber, G. L. Kane and S. Dawson, Front. Phys. **80** (2000) 1.
 - [19] G. C. Branco *et al.*, Phys. Rept. **516** (2012) 1.
 - [20] K. -m. Cheung, hep-ph/9507411.
 - [21] M. Spira and J. D. Wells, Nucl. Phys. B **523** (1998) 3.

- [22] B. Lillie, J. Shu and T. M. P. Tait, JHEP **0804** (2008) 087.
- [23] C. R. Chen, W. Klemm, V. Rentala and K. Wang, Phys. Rev. D **79** (2009) 054002.
- [24] V. Barger, W. Y. Keung and B. Yencho, Phys. Lett. B **687** (2010) 70.
- [25] S. Jung and J. D. Wells, JHEP **1011** (2010) 001.
- [26] G. Cacciapaglia, R. Chierici, A. Deandrea, L. Panizzi, S. Perries and S. Tosi, JHEP **1110** (2011) 042.
- [27] T. Gregoire, E. Katz and V. Sanz, Phys. Rev. D **85** (2012) 055024.
- [28] J. A. Aguilar-Saavedra and J. Santiago, Phys. Rev. D **85** (2012) 034021.
- [29] C. Han, N. Liu, L. Wu and J. M. Yang, Phys. Lett. B **714** (2012) 295.
- [30] C. R. Chen, Phys. Lett. B **736** (2014) 321.
- [31] P. S. B. Dev and A. Pilaftsis, JHEP **1412** (2014) 024.
- [32] N. Greiner, K. Kong, J. C. Park, S. C. Park and J. C. Winter, JHEP **1504** (2015) 029.
- [33] L. Beck, F. Blekman, D. Dobur, B. Fuks, J. Keaveney and K. Mawatari, arXiv:1501.07580 [hep-ph].
- [34] N. Craig, F. D'Eramo, P. Draper, S. Thomas and H. Zhang, arXiv:1504.04630 [hep-ph].
- [35] A. Djouadi, H. E. Haber and P. M. Zerwas, Phys. Lett. B **375** (1996) 203.
- [36] J. F. Gunion, L. Roszkowski, A. Turski, H. E. Haber, G. Gamberini, B. Kayser, S. F. Novaes and F. I. Olness *et al.*, Phys. Rev. D **38** (1988) 3444.
- [37] F. Borzumati, J. -L. Kneur and N. Polonsky, Phys. Rev. D **60** (1999) 115011.
- [38] T. Plehn, Phys. Rev. D **67** (2003) 014018;
E. L. Berger, T. Han, J. Jiang and T. Plehn, Phys. Rev. D **71** (2005) 115012.
- [39] S. Kanemura, S. Moretti and K. Odagiri, JHEP **0102** (2001) 011.
- [40] S. Moretti, Eur. Phys. J. direct C **4** (2002) 15.
- [41] S. Kiyoura, S. Kanemura, K. Odagiri, Y. Okada, E. Senaha, S. Yamashita and Y. Yasui, hep-ph/0301172.
- [42] V. D. Barger, J. L. Hewett and R. J. N. Phillips, Phys. Rev. D **41** (1990) 3421.
- [43] Y. Grossman, Nucl. Phys. B **426** (1994) 355.
- [44] M. Aoki, S. Kanemura, K. Tsumura and K. Yagyu, Phys. Rev. D **80** (2009) 015017.
- [45] S. L. Glashow and S. Weinberg, Phys. Rev. D **15** (1977) 1958.
- [46] S. Kanemura, T. Kubota and E. Takasugi, Phys. Lett. B **313** (1993) 155.
- [47] A. G. Akeroyd, A. Arhrib and E. -M. Naimi, Phys. Lett. B **490** (2000) 119.

- [48] I. F. Ginzburg and I. P. Ivanov, Phys. Rev. D **720** (2005) 11501.
- [49] N. G. Deshpande and E. Ma, Phys. Rev. D **18** (1978) 2574.
- [50] S. Kanemura, T. Kasai and Y. Okada, Phys. Lett. B **471** (1999) 182.
- [51] S. Nie and M. Sher, Phys. Lett. B **449** (1999) 89.
- [52] J. F. Gunion and H. E. Haber, Phys. Rev. D **67** (2003) 075019.
- [53] S. Kanemura and C. P. Yuan, Phys. Lett. B **530** (2002) 188.
- [54] Q. H. Cao, S. Kanemura and C. P. Yuan, Phys. Rev. D **69** (2004) 075008.
- [55] A. Djouadi, Phys. Rept. **457** (2008) 1; Phys. Rept. **459** (2008) 1.
- [56] J. Alwall, M. Herquet, F. Maltoni, O. Mattelaer and T. Stelzer, JHEP **1106** (2011) 128.
- [57] J. Pumplin, D. R. Stump, J. Huston, H. L. Lai, P. M. Nadolsky and W. K. Tung, JHEP **0207** (2002) 012.
- [58] The ATLAS collaboration, ATLAS-CONF-2013-051, ATLAS-COM-CONF-2013-055.
- [59] V. Khachatryan *et al.* [CMS Collaboration], JHEP **1411** (2014) 154.
- [60] G. Bevilacqua and M. Worek, JHEP **1207** (2012) 111.
- [61] F. Mahmoudi and O. Stal, Phys. Rev. D **81** (2010) 035016.
- [62] X. D. Cheng, Y. D. Yang and X. B. Yuan, Eur. Phys. J. C **74**, no. 10 (2014) 3081.
- [63] T. Sjostrand, S. Mrenna and P. Z. Skands, JHEP **0605** (2006) 026.
- [64] S. Jadach, Z. Was, R. Decker and J. H. Kuhn, Comput. Phys. Commun. **76** (1993) 361.
- [65] R. Yonamine, K. Ikematsu, T. Tanabe, K. Fujii, Y. Kiyo, Y. Sumino and H. Yokoya, Phys. Rev. D **84** (2011) 014033.
- [66] S. Catani, Y. L. Dokshitzer, M. Olsson, G. Turnock and B. R. Webber, Phys. Lett. B **269** (1991) 432.
- [67] M. Cacciari, G. P. Salam and G. Soyez, Eur. Phys. J. C **72** (2012) 1896.
- [68] S. Kanemura, K. Tsumura and H. Yokoya, Phys. Rev. D **85** (2012) 095001.
- [69] S. Kanemura, K. Tsumura and H. Yokoya, Phys. Rev. D **88** (2013) 055010.
- [70] M. Battaglia and G. Servant, Nuovo Cim. C **033N2** (2010) 203.